THE JOURNAL OF BIOLOGICAL CHEMISTRY VOL. 287, NO. 43, pp. 36291–36304, October 19, 2012

Protein Kinase N1 Is a Novel Substrate of NFATc1-mediated Cyclin D1-CDK6 Activity and Modulates Vascular Smooth Muscle Cell Division and Migration Leading to Inward Blood Vessel Wall Remodeling*

Received for publication, March 15, 2012, and in revised form, August 7, 2012 Published, JBC Papers in Press, August 13, 2012, DOI 10.1074/jbc.M112.361220

Nikhlesh K. Singh[‡], Venkatesh Kundumani-Sridharan[‡], Sanjay Kumar[‡], Shailendra K. Verma[‡], Sivareddy Kotla[‡], Hideyuki Mukai[§], Mark R. Heckle[‡], and Gadiparthi N. Rao[‡1]

From the [‡]Department of Physiology, University of Tennessee Health Science Center, Memphis, Tennessee 38163 and the [§]Biosignal Research Center, Kobe University, Kobe 657-8501, Japan

Background: The purpose of this study was to test the role of PKN1 in vascular wall remodeling.
Results: PKN1 mediates MCP-1-induced HASMC migration/proliferation and balloon injury-induced neointima formation.
Conclusion: PKN1 plays a role in vascular wall remodeling following balloon injury.
Significance: PKN1 could be a promising target for the next generation of drugs for vascular diseases such as restenosis.

Toward understanding the mechanisms of vascular wall remodeling, here we have studied the role of NFATc1 in MCP-1-induced human aortic smooth muscle cell (HASMC) growth and migration and injury-induced rat aortic wall remodeling. We have identified PKN1 as a novel downstream target of NFATc1-cyclin D1/CDK6 activity in mediating vascular wall remodeling following injury. MCP-1, a potent chemoattractant protein, besides enhancing HASMC motility, also induced its growth, and these effects require NFATc1-dependent cyclin D1 expression and CDK4/6 activity. In addition, MCP-1 induced PKN1 activation in a sustained and NFATc1-cyclin D1/CDK6-dependent manner. Furthermore, PKN1 activation is required for MCP-1-induced HASMC growth and migration. Balloon injury induced PKN1 activation in NFAT-dependent manner and pharmacological or dominant negative mutant-mediated blockade of PKN1 function or siRNA-mediated down-regulation of its levels substantially suppressed balloon injury-induced smooth muscle cell migration and proliferation resulting in reduced neointima formation. These novel findings suggest that PKN1 plays a critical role in vascular wall remodeling, and therefore, it could be a promising new target for the next generation of drugs for vascular diseases, particularly restenosis following angioplasty, stent implantation, or vein grafting.

Restenosis, characterized by thickening of the arterial wall, is believed to be a multifactorial disease that occurs as a response to injury (1). Among many cell types, smooth muscle cells have been shown to contribute profoundly to the pathogenesis of this vascular disease (2). In addition, in recent years many reports showed that progenitor cell recruitment to and homing at the site of vascular injury play a role in this disease pathogenesis (3). A variety of biomolecules produced at the site of vascular injury appear to be involved in the pathogenesis of restenosis (2). Among the many molecules identified, the artery produces monocyte chemotactic protein-1 (MCP-1) very acutely and robustly in response to injury (4). MCP-1 also known as chemokine (C-C motif) ligand 2 (CCL2) belongs to CC chemokine family and it recruits monocytes, memory T cells, and dendritic cells to the sites of tissue injury, infection, and inflammation (5, 6). Although some controversy exists in regard to the role of MCP-1 in VSMC[2] mitogenesis (7), emerging evidence points out that it plays a major role in vascular inflammation and possesses the capacity to stimulate VSMC growth and thereby contribute to vascular wall remodeling (8–10). Earlier, we have reported that 15-lipoxygenase 1–15(*S*)-hydroxyeicosatetraenoic acid axis induces the expression of MCP-1 via a mechanism involving epidermal growth factor receptor, Src, Jak2, and STAT-3 in intact artery in response to injury and mediates SMC migration leading to neointima formation (11, 12). NFATs consisting of NFATc1–c4 and NFAT5 are members of a multigene family of transcription factors that belong to the Rel group (13). Structure and function studies have identified a transcription activation domain in the N-terminal region of NFATs (13). NFATc1–c4 contain a conserved serine-repeat regulatory region adjacent to the transcription activation domain. This region also includes the calcineurin-binding sites. The C-terminal region contains a Rel homology domain that mediates NFAT DNA binding (13). Dephosphorylation of NFATs, which is mediated by a Ca^{2+}/calmodulin-dependent phosphatase, calcineurin, leads to their activation and nuclear translocation (14). However, phosphorylation by kinases such as glycogen synthase kinase 3β (GSK3β) invokes their nuclear export and inactivation (15). NFATs bind to the GGAAA core DNA element present in the promoter regions of the genes and influ-

* This work was supported, in whole or in part, by National Institutes of Health Grants HL069908 and HL103575 from the NHLBI (to G. N. R.).
[1] To whom correspondence should be addressed: Dept. of Physiology, University of Tennessee Health Science Center, 894 Union Ave., Memphis, TN 38163. Tel.: 901-448-7321; Fax: 901-448-7126; E-mail: rgadipar@uthsc.edu.

[2] The abbreviations used are: VSMC, vascular smooth muscle cell; HASMC, human aortic smooth muscle cell; NFAT, nuclear factor of activated T-cell; SMC, smooth muscle cell; BI, balloon injury; I/M, intimal/medial ratio; Rb, retinoblastoma protein.

ence their transcription. In addition to their role in cytokine gene regulation in immune cells, a number of studies using knock-out mouse models have revealed that these transcriptional factors play an important role in the development of the cardiovascular system as well as in the pathological cardiac hypertrophy (16–19). The work from our laboratory showed that these transcriptional factors are involved in the regulation of VSMC growth and migration (20, 21). The most exciting findings in this aspect are our recent observations that the blockade of NFATs inhibits balloon injury-induced VSMC migration, proliferation, and neointima formation (22). In understanding the mechanisms of NFAT involvement in vascular wall remodeling, we found that NFATc1 targets cyclins, particularly cyclin D1 and cyclin A2, in modulating both VSMC growth and migration (23, 24). Thus, these findings provide strong evidence for the role of NFATs in receptor tyrosine kinase and G protein-coupled receptor agonist-induced VSMC growth and migration *in vitro* and injury-induced neointima formation *in vivo*. However, targeting these transcriptional factors for drug discovery needs more extensive work to find whether they play a unifying role in the regulation of VSMC growth and motility in response to many cues. This study was undertaken to test whether NFATs mediate the effects of MCP-1 in vascular wall remodeling and, if so, to identify the underlying mechanisms.

MATERIALS AND METHODS

Reagents—Cyclosporin A (A-195) and Ro318220 (BML-EI282-0001) were bought from ENZO Life Sciences (Plymouth Meeting, PA). Pluronic F127 (P2443) and anti-smooth muscle α-actin antibodies (A2547) were purchased from Sigma. Recombinant human MCP-1 (279-MC) was from R & D Systems Inc. (Minneapolis, MN). Anti-CDK4 (SC-260), anti-CDK6 (SC-56362), anti-β-tubulin (SC-9104), anti-GFP (SC-9996), anti-MEK1 (SC-219), anti-p53 (SC-6243), anti-PKN1 (SC-136037), and anti-PKN3 (SC-67770) antibodies and truncated Rb protein (SC-4112) were obtained from Santa Cruz Biotechnology, Inc. (Santa Cruz, CA). Anti-Ki67 (ab15580) and anti-Ser(P)/Thr(P) (ab17464) antibodies were purchased from Abcam (Cambridge, MA). Anti-cyclin D1 antibody (RB-010-P) was bought from NeoMarkers (Fremont, CA). Anti-NFATc1 antibody (MA3–024) was from Affinity BioReagents (Golden, CO). Anti-pPKN1 (2611) and anti-PKN2 (2612) antibodies were obtained from Cell Signaling Technology (Beverly, MA). The ABC kit, DAB kit, and Vectashield mounting medium were bought from Vector Laboratories Inc. (Burlingame, CA). Hoechst 33342 (3570), Lipofectamine 2000 reagent, Prolong Gold antifade mounting medium (P36930), and recombinant full-length PKN1 protein (PV3790) were obtained from Invitrogen. [γ-^{32}P]ATP (specific activity 3000 Ci/mmol) was from MP Biomedicals (Irvine, CA). [^{3}H]Thymidine (specific activity 20 Ci/mmol) was obtained from PerkinElmer Life Sciences. Protein A-Sepharose (CL-4B) and protein G-Sepharose were purchased from Amersham Biosciences. Human NFATc1 siRNA (ON-TARGETplus SMARTpool L-003605-00, NM_172390), human cyclin D1 siRNA (ON-TARGETplus SMARTpool L-003210-00, NM-053056), human CDK4 siRNA (ON-TARGETplus SMARTpool L-003238-00, NM_000075), human CDK6 siRNA (ON-TARGETplus SMARTpool L-003240-00, NM_001259), human PKN1 siRNA (ON-TARGETplus SMARTpool L-004175-00, NM_005585), rat PKN1 siRNA (ON-TARGETplus SMARTpool L-090263-00, NM_029355), human NFATc1 siRNA (siGENOME siRNA D-003605-23), human cyclin D1 siRNA (siGENOME siRNA D-003210-07), human CDK6 siRNA (siGENOME siRNA D-003240-09), and control nontargeting siRNA (D-001810-10) were bought from Dharmacon RNAi Technologies (Chicago). The ECL Western blotting detection reagents (catalog no. RPN2106) were obtained from GE Healthcare.

Adenoviral Vectors—The generation of pR1445 encoding the human PKN1 catalytic domain (amino acids 560–950) with K644E mutation was described previously (25). To construct an adenoviral vector, the mutant catalytic domain of PKN1 was amplified using the following primers: forward, 5′-CTGGggtaccGTCGACATGGACAGCTCACCTCAGAAG-3′ incorporating a KpnI restriction enzyme site at the 5′-end, and reverse, 5′-CACCctcgagACTAGTGGATCCCCCGGGCTGCAGG-3′ incorporating an XhoI restriction enzyme site at the 5′-end and pR1445 as a template. The PCR products were digested with KpnI and XhoI, and the released fragment was cloned into KpnI and XhoI sites of the pENTR3C vector (Invitrogen) to yield pENTR3C-dnPKN1 vector. The pAd-dnPKN1 was generated by recombination between pENTR3C-dnPKN1 and pAdCMVV5DEST (Invitrogen) and verified by DNA sequencing. The pAd-dnPKN1 was linearized with PacI and transfected into HEK293A cells. The resulting adenovirus was further amplified by infection of HEK293A cells and purified by cesium chloride gradient ultracentrifugation as described previously (22). Construction of Ad-GFP and Ad-GFPVIVIT was also described previously (22).

Cell Culture—HASMCs were purchased from Cascade Biologicals (Portland, OR), subcultured in Medium 231 containing smooth muscle cell growth supplements, and used between 4 and 10 passages.

Transfections and Transductions—HASMCs were transfected with siRNA molecules at a final concentration of 100 nM using Lipofectamine 2000 transfection reagent according to the manufacturer's instructions. When adenoviral vectors were used to block the function of a specific molecule, cells were transduced with adenovirus harboring either GFP or dominant negative mutants of the target molecule at 40 multiplicities of infection overnight in complete medium. After transfections or transductions, cells were growth-arrested for 36 h and used as required.

CDK4/6 and PKN1 Assays—Protein extracts from cells or tissues were analyzed for CDK4/6 and/or PKN1 activities as described previously (26, 27). The ^{32}P-labeled Rb protein, PKN1, and/or MBP were visualized by autoradiography, and the band intensities were quantified using Image J (National Institutes of Health).

DNA Synthesis—DNA synthesis was measured by [^{3}H]thymidine incorporation as described previously and expressed as counts/min/dish (28).

Cell Migration—Cell migration was measured using a modified Boyden chamber method as described previously (29). Cell motility is presented as number of migrated cells/field.

Western Blot Analysis—After appropriate treatments, cell or tissue extracts were prepared, and an equal amount of protein from control and each treatment was analyzed by Western blotting for the indicated molecule using its specific antibody as described previously (23). The band intensities were quantified using Image J (National Institutes of Health).

Common Carotid Artery BI—All animal protocols were performed in accordance with the relevant guidelines and regulations approved by the Institutional Animal Care and Use Committee of the University of Tennessee Health Science Center, Memphis. Sprague-Dawley male rats weighing ~300–350 g were used throughout the study. BI and adenoviral transductions were performed essentially as described previously (30). To deliver the pharmacological PKN1 inhibitor, Ro318220, into the artery, it was prepared in DMSO, mixed with 30% pluronic gel, and applied around the injured artery as described by Subramanian *et al.* (31). In the case of delivering siRNA molecules into the artery, control or targeting siRNA along with Lipofectamine 2000 reagent were mixed in 30% pluronic gel and applied around the injured artery. At 1, 3, and 5 days and 1 or 2 weeks after BI, the animals were sacrificed by CO_2 inhalation followed by thoracotomy, and the common carotid arteries were collected and processed for protein extraction and/or immunohistological staining.

In Vivo Smooth Muscle Cell Migration Assay—The *in vivo* SMC migration was determined as described by Bendeck *et al.* (32). Briefly, 3 days after BI, the carotid arteries were fixed *in vivo* with 10% buffered formalin at physiological pressure. The middle 1 cm of the denuded (injured) common carotid artery was cut and fixed in cold acetone for 10 min. The artery was then opened longitudinally and pinned down onto an agar plate with the luminal surface facing upward. The arteries were rinsed in PBS and then placed in 0.3% H_2O_2 for 30 min to block endogenous peroxidase activity. Nonspecific protein binding was blocked by incubating the arteries in 5% normal goat serum in PBS for 30 min. The arteries were incubated with anti-SMCα-actin antibodies diluted 1:300 in PBS for 1 h followed by incubation with biotinylated goat anti-mouse IgG for 30 min. Peroxidase labeling was carried out by using ABC kit (Vector Laboratories), and the signals were visualized by using DAB kit (Vector Laboratories). After each step, the slides were rinsed three times for 5 min each in PBS. Finally, the opened arteries were placed intimal side up on glass slides with coverslips. As a negative control, samples of the same specimens without the primary antibody incubation were used. The intimal surface of the vessel was examined under a light microscope at ×200 magnification, and SMCα-actin-positively stained cells were counted.

Double Immunofluorescence Staining—Soon after isolation, the injured common carotid arteries were snap-frozen in OCT compound (Sakura Finetek USA Inc., Torrance, CA). Cryosections (5 μm) were made using Leica Cryostat (Model CM3050S, Leica, Wetzlar, Germany). After blocking in goat serum, the cryosections were incubated with rabbit anti-rat Ki67 antibodies and mouse anti-rat SMCα-actin antibodies for 1 h. After washing in PBS, all slides were incubated with goat anti-rabbit secondary antibodies conjugated with Alexa Fluor 568 and goat anti-mouse secondary antibodies conjugated with Alexa Fluor 488. Fluorescence was observed under Zeiss Axio Observer Z1 motorized inverted microscope. Negative controls were processed exactly as described above except that they were not incubated with primary antibodies.

Histological Staining—For morphometric analysis, the injured common carotid arteries were fixed in 10% formalin, dehydrated, and embedded in OCT compound. The sections were made as described above and stained with hematoxylin and eosin. The intimal (I) and medial (M) areas were measured using ImageJ (National Institutes of Health), and the I/M ratios were calculated.

Statistics—All the experiments were repeated three times with similar results. Data are presented as the means ± S.D. The control *versus* treatment effects were analyzed by two-tailed Student's *t* test, and p values <0.05 were considered to be statistically significant. In the case of Western blotting, immunohistochemistry, and CDK4/6 and PKN1 activities, one set of the representative data is shown.

RESULTS

NFATc1 Mediates MCP-1-induced HASMC DNA Synthesis and Migration—Previously, we have reported that 15-lipoxygenase 1–15(*S*)-hydroxyeicosatetraenoic acid-induced VSMC migration both *in vitro* and *in vivo* requires MCP-1 production (12). We have also demonstrated that NFATc1 mediates PDGF-BB-induced HASMC migration and proliferation (23, 24). Therefore, we asked the question whether MCP-1 modulates the migration and proliferation of HASMCs, and if so, what is the role of NFATs in these effects. MCP-1 induced HASMC migration and proliferation in a dose-dependent manner with maximum effects at 50 ng/ml (Fig. 1, *A* and *B*). To test the role of NFATs in these responses, we first studied the effect of MCP-1 on NFATc1 activation in HASMCs. MCP-1 (50 ng/ml) induced NFATc1 stimulation as measured by its translocation from the cytoplasm to the nucleus in a time-dependent manner in HASMCs (Fig. 1*C*), and cyclosporin A, a potent inhibitor of calcineurin (13), blocked MCP-1-induced NFATc1 translocation (Fig. 1*D*). In addition, either blockade of NFAT activation by VIVIT, a pentapeptide that competes with NFATs for binding to calcineurin (33), or down-regulation of NFATc1 levels using its siRNA attenuated MCP-1 induced HASMC DNA synthesis and migration (Fig. 1, *E–H*). These results indicate that NFATc1 plays a role in MCP-1-induced DNA synthesis and migration.

Both Cyclin D1-dependent CDK4 and CDK6 Activities Are Required for MCP-1-induced HASMC DNA Synthesis and Migration Downstream to NFATc1—In our previous study, we demonstrated that NFATc1 mediates PDGF-BB-induced cyclin D1 expression (23). To test whether MCP-1 induces cyclin D1 expression, and if so, the role of NFATc1, we first studied the time course effect of MCP-1 on cyclin D1 expression. MCP-1 induced cyclin D1 expression in a time-dependent manner with a maximum effect at 4 and 8 h (Fig. 2*A*). Because cyclin D1 binds to CDK4–6 and forms their respective holoenzymes, we next studied the time course effect of MCP-1 on CDK activities, particularly CDK4 and CDK6. Consistent with its effect on cyclin D1 expression, MCP-1 induced both CDK4 and CDK6 activities with maximum effects at 4 and 8 h (Fig.

2*B*). Furthermore, down-regulation of cyclin D1 levels by its siRNA inhibited MCP-1-induced CDK4 and CDK6 activities (Fig. 2*C*). This finding indicates that cyclin D1 expression is needed for MCP-1-induced CDK4 and CDK6 activities. Using the siRNA approach, we next examined their role in MCP-1-induced HASMC growth and migration. Down-regulation of either cyclin D1 or CDK4/6 levels by their respective siRNA molecules blocked both MCP-1-induced HASMC DNA synthesis and migration (Fig. 3, *A–D*). To understand the mechanisms by which MCP-1 induces cyclin D1 expression and CDK4/6 activities, we have studied the role of NFATs. Inhibition of NFAT activation by VIVIT or down-regulation of NFATc1 lev-

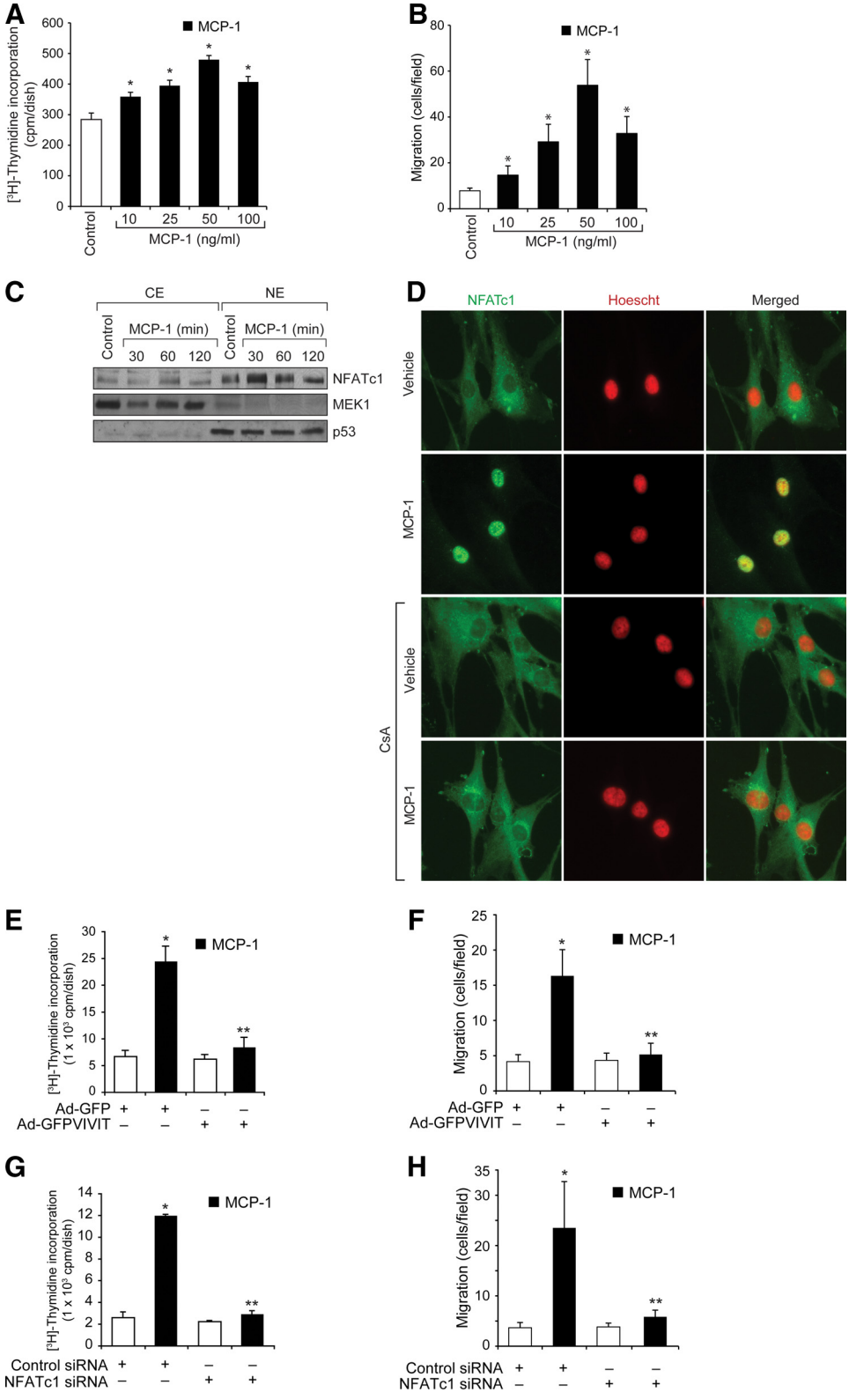

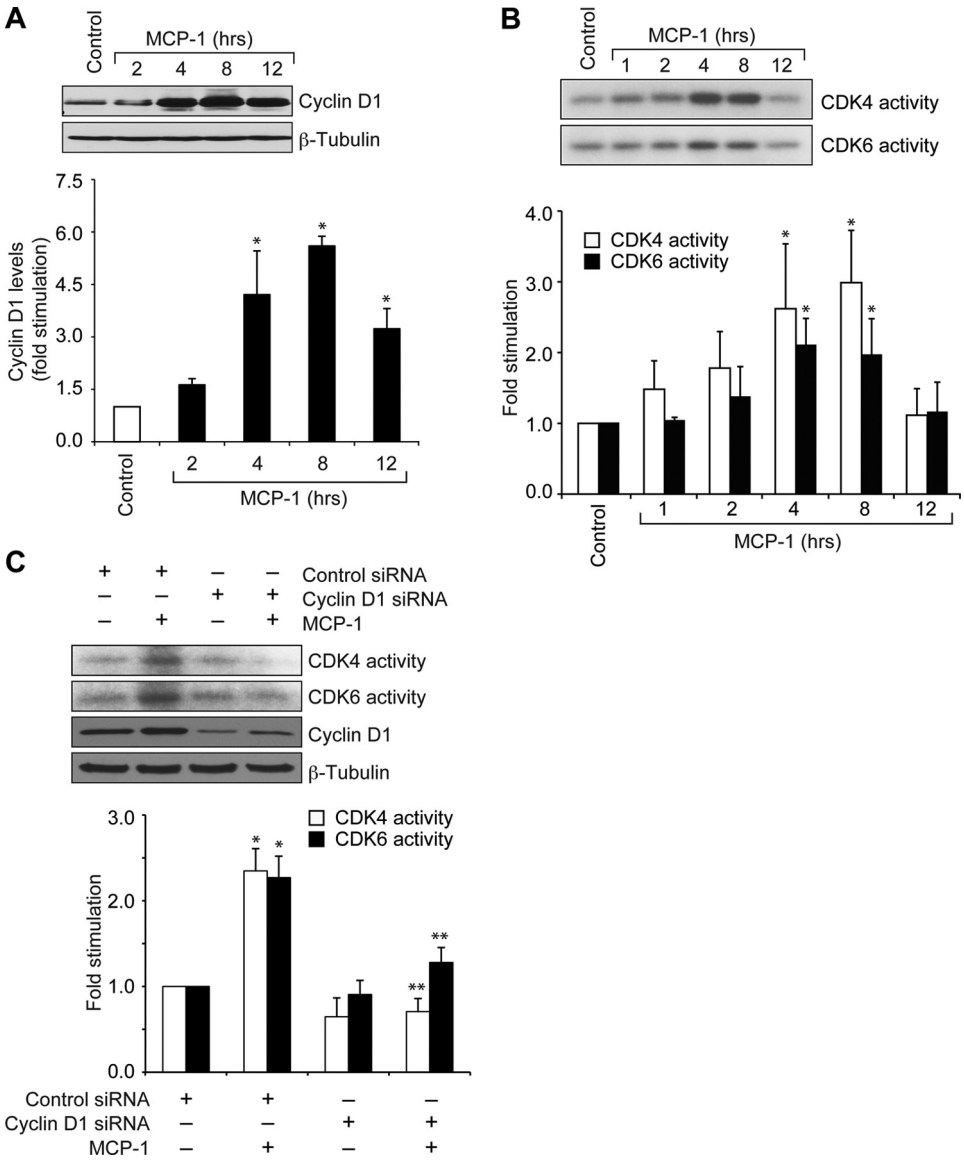

FIGURE 2. **MCP-1 induces cyclin D1 expression and CDK4/6 activities in HASMCs.** *A* and *B,* quiescent HASMCs were treated with and without MCP-1 (50 ng/ml) for the indicated time periods, and cell extracts were prepared. An equal amount of protein from control and each treatment was analyzed by Western blotting for cyclin D1 levels using its specific antibodies (*A*) or immunocomplex kinase assay for CDK4/6 activities using truncated recombinant retinoblastoma protein and [γ-^{32}P]ATP as substrates (*B*). The blot in *A* was reprobed with anti-β-tubulin antibodies to show the lane loading control. *C,* after transfecting with either control or cyclin D1 siRNA (100 nM) and quiescence, HASMCs were treated with and without MCP-1 (50 ng/ml) for 8 h; cell extracts were prepared and analyzed by immunocomplex kinase assay for CDK4/6 activities as described in *B*. Total cellular extracts containing an equal amount of protein from control and each treatment were analyzed by Western blotting sequentially for cyclin D1 and β-tubulin levels to show the effects of cyclin D1 siRNA on its target and nontarget gene expressions. *, $p < 0.01$ *versus* vehicle control or control siRNA; **, $p < 0.01$ *versus* control siRNA + MCP-1.

els by its siRNA suppressed MCP-1-induced cyclin D1 expression and CDK4/6 activities (Fig. 4, *A–D*). These results suggest that NFATc1 mediates MCP-1-induced cyclin D1 expression and CDK4/6 activities in HASMCs.

MCP-1 Induces PKN1 Phosphorylation and Activity in NFATc1 and Cyclin D1-CDK6-dependent Manner—It was well established that Rho GTPases such as RhoA and Rac1 play an important role in cell migration and proliferation (34, 35). In

FIGURE 1. **NFATc1 mediates MCP-1-induced HASMC proliferation and migration.** *A* and *B,* quiescent HASMCs were treated with and without the indicated doses of MCP-1 for 24 and 8 h to measure DNA synthesis and cell migration, respectively. Cell migration was measured by Boyden chamber method, and DNA synthesis was measured by [^{3}H]thymidine incorporation. *C,* quiescent HASMCs were treated with and without MCP-1 (50 ng/ml) for the indicated time periods, and cytoplasmic and nuclear extracts were prepared. An equal amount of protein from control and each treatment was analyzed by Western blotting for NFATc1 levels using its specific antibodies. The blot was reprobed sequentially with anti-MEK1 and anti-p53 antibodies to show the relative purity of the cytoplasmic and nuclear extracts. *D,* quiescent HASMCs were treated with and without MCP-1 (50 ng/ml) in the presence and absence of 10 μM cyclosporin A (*CsA*) for 30 min, fixed, permeabilized, and immunostained for NFATc1 using its specific antibodies followed by probing with Alexa Fluor 488-conjugated secondary antibodies. *E* and *F,* HASMCs that were transduced with either Ad-GFP or Ad-GFPVIVIT at 40 multiplicities of infection and quiesced were treated with and without MCP-1 (50 ng/ml) for either 24 h to determine DNA synthesis (*E*) or 8 h to measure cell migration (*F*). *G* and *H,* after transfection with control or NFATc1 siRNA (100 nM) and quiescence, HASMC DNA synthesis and migration were measured in response to MCP-1 as described in *A* and *B*, respectively. *CE,* cytoplasmic extract; *NE,* nuclear extract. *, $p < 0.01$ *versus* vehicle control, Ad-GFP or control siRNA; **, $p < 0.01$ *versus* Ad-GFP + MCP-1 or control siRNA + MCP-1.

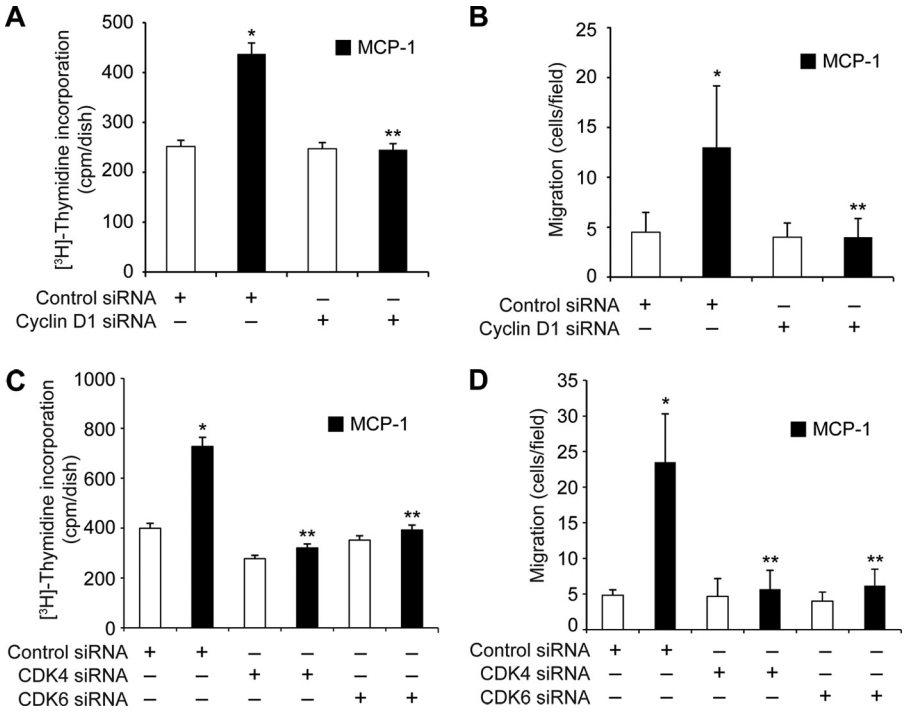

FIGURE 3. **Cyclin D1 and CDK4/6 activities are required for MCP-1-induced HASMC proliferation and migration.** *A–D,* after transfection with control, cyclin D1, CDK4, or CDK6 siRNA (100 nM) and quiescence, HASMCs were subjected to MCP-1-induced DNA synthesis (*A* and *C*) or migration (*B* and *D*). *, $p < 0.01$ *versus* control siRNA; **, $p < 0.01$ *versus* control siRNA + MCP-1.

addition, it was reported that these Rho GTPases regulate protein kinase N1 (PKN1) in mediating cytoskeleton organization (36, 37). Because MCP-1 is a potent chemotactic protein, we wanted to find out whether it has any effect on PKN1 activation. PKN1 activation requires phosphorylation at Thr-774 (37). Therefore, we measured PKN1 Thr-774 phosphorylation. To our surprise, MCP-1 induced the activation of PKN1 but not PKN2/3 in a time-dependent manner in HASMCs with a maximum effect at 4 and 8 h (Fig. 5*A*). Furthermore, depletion of PKN1 levels by its siRNA blocked MCP-1-induced HASMC DNA synthesis and migration (Fig. 5, *B* and *C*), suggesting that PKN1 plays an important role in MCP-1-induced HASMC growth and migration. To explore the mechanism of PKN1 activation by MCP-1, we have studied the role of NFATc1, cyclin D1, and CDK4/6. Depletion of NFATc1, cyclin D1, or CDK6 but not CDK4 levels abolished MCP-1-induced PKN1 phosphorylation (Fig. 5, *D–F*). To ascertain that PKN1 phosphorylation leads to its activation, we measured its kinase activity. MCP-1 induced PKN1 activity in a time-dependent manner (Fig. 5*G*). In addition, siRNA-mediated depletion of NFATc1, cyclin D1, or CDK6 levels blocked MCP-1-induced PKN1 activity (Fig. 5*G*). To confirm the role of NFATc1, cyclin D1, and CDK6 in MCP-1-induced PKN1 activation, we also used siGENOME siRNA molecules, which are distinct from ON-TARGETplus SMARTpool siRNAs, to deplete their levels. Down-regulation of NFATc1, cyclin D1, and CDK6 by their respective siGENOME siRNA molecules also attenuated MCP-1-induced PKN1 phosphorylation and activity (Fig. 5*G*). Because cyclin D1-CDK6 modulated MCP-1-induced PKN1 activation, we next examined whether these molecules physically interact with each other by co-immunoprecipitation. We found that although CDK6 and PKN1 exist as a complex even in quiescent cells, cyclin D1 was found to be associated with this complex in an inducible manner in response to MCP-1 (Fig. 6*A*). Similarly, increases in the association of pPKN1 and CDK6 with cyclin D1 were also observed in response to MCP-1 (Fig. 6*A*). Because PKN1 was found to be associated with CDK6 and cyclin D1, we asked whether PKN1 is a substrate for CDK6. To address this question, quiescent HASMCs were treated with and without MCP-1 (50 ng/ml) for 8 h, and cell extracts were prepared. An equal amount of protein from control and MCP-1-treated HASMCs was immunoprecipitated with anti-CDK6 antibodies, and the immunocomplexes were subjected to immunocomplex kinase assay using recombinant full-length PKN1 and [γ-^{32}P]ATP as substrates. As shown in Fig. 6*B*, CDK6 phosphorylated PKN1, and this phosphorylation was found to be 2–3-fold more in response to MCP-1 treatment as compared with control. Together, these observations revealed that MCP-1 activates PKN1 in NFATc1-cyclin D1-CDK6-dependent manner mediating HASMC growth and migration.

PKN1 Mediates BI-induced SMC Migration, Proliferation, and Neointima Formation—To find whether arterial injury stimulates PKN1, and if so, the potential role of the NFATc1-cyclin D1-CDK6 axis, we used the rat carotid artery restenosis model. We measured cyclin D1 expression, CDK6 activity, and PKN1 phosphorylation/activity in carotid arteries at 1, 3, and 5 days after vascular injury. BI induced cyclin D1 expression and CDK6 activity in a time-dependent manner with a maximum effect at 3 days post injury (Fig. 7*A*). BI also induced PKN1 phosphorylation and activity with maximum effects at 5 days post-injury (Fig. 7*A*). To test whether BI-induced PKN1 activation requires the NFAT-cyclin D1-CDK6 axis, we studied the effect of VIVIT. Adenovirus-mediated transduction of VIVIT blocked BI-induced cyclin D1 expression, CDK6 activity, and

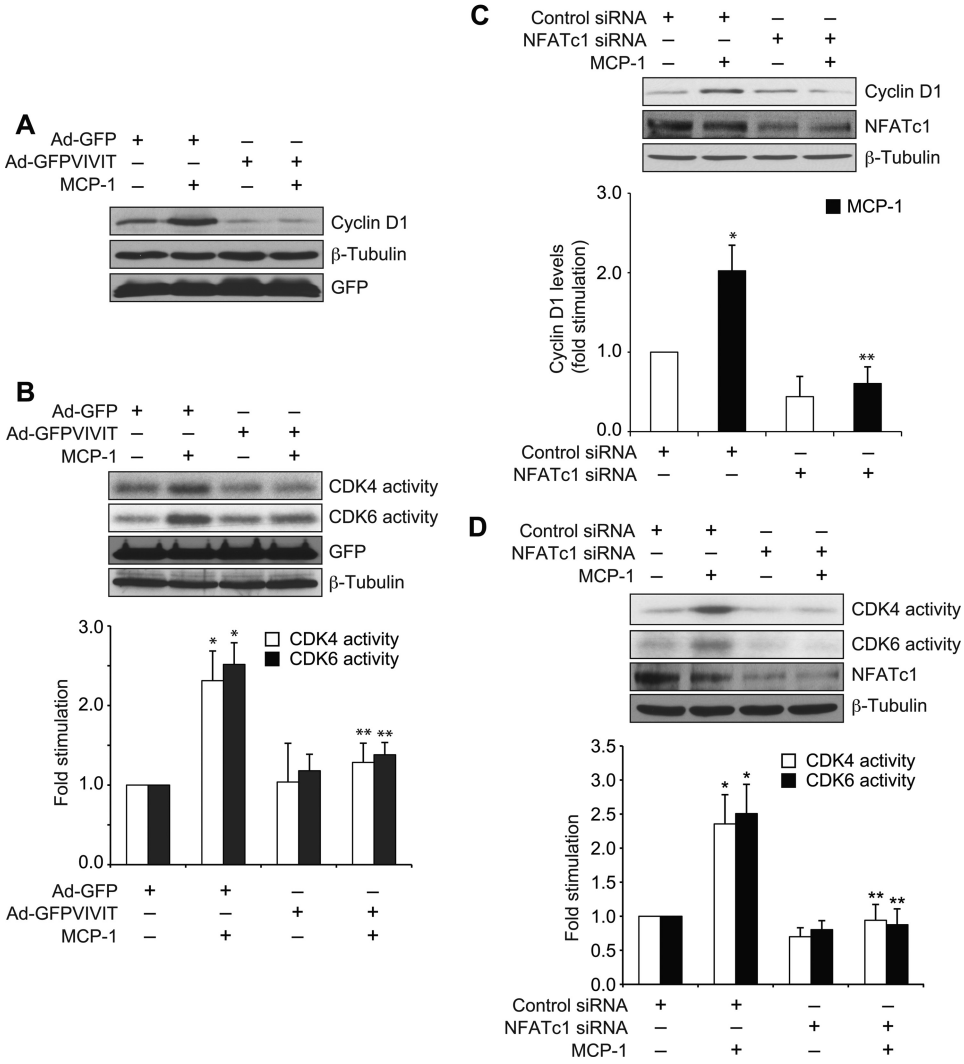

FIGURE 4. **NFATc1 mediates MCP-1-induced cyclin D1 expression and CDK4/6 activities in HASMCs.** *A–D,* HASMCs that were transduced with Ad-GFP or Ad-GFPVIVIT (40 multiplicities of infection) or transfected with control or NFATc1 siRNA (100 nM) and quiesced were treated with and without MCP-1 (50 ng/ml) for 8 h, and cell extracts were prepared and analyzed for cyclin D1 levels and CDK4/6 activities as described in Fig. 2, *A* and *B*, respectively. The blots in *A* and *C* were reprobed sequentially for GFP, β-tubulin or NFATc1 levels using their respective antibodies to show the expression of the vector, lane loading control, or NFATc1 siRNA effect on its target and nontarget gene expressions. The blots for GFP, β-tubulin, or NFATc1 levels in *B* and *D* show the vector expression, normalization, or NFAT siRNA on its target and nontarget gene expressions in the total cell extracts. The *bar graph* in each panel represents the quantitative analysis of three independent experiments. *, $p < 0.01$ *versus* Ad-GFP or control siRNA; **, $p < 0.01$ *versus* Ad-GFP + MCP-1 or control siRNA + MCP-1.

PKN1 phosphorylation/activity (Fig. 7*B*). To study the role of PKN1 in vascular wall remodeling, we examined the effect of Ro318220, a potent inhibitor of PKN1 (38), on BI-induced SMC migration, proliferation, and neointima formation. Ro318220 blocked BI-induced SMC migration, proliferation, and neointima formation (Fig. 7, *C–E*). To confirm the role of PKN1 in vascular wall remodeling, we also used the siRNA approach. Pluronic gel (30%, v/v)-mediated delivery of PKN1 siRNA (10 μg) mixed with Lipofectamine 2000 reagent into the artery depleted PKN1 levels substantially in the artery and attenuated BI-induced SMC migration, proliferation, and neointima formation (Fig. 8, *A–D*). Similarly, adenovirus-mediated transduction of dnPKN1 also inhibited BI-induced SMC migration, proliferation, and neointima formation (Fig. 9, *A–D*).

DISCUSSION

The important findings of this study are as follows. 1) MCP-1, a potent chemotactic protein, stimulated both growth and migration of HASMCs, 2) MCP-1 activated NFATc1 in a time-dependent manner in HASMCs, 3) Both MCP-1-induced HASMC growth and migration require NFATc1 activation. 4) MCP-1 induced cyclin D1 expression and CDK4/6 activities in an NFATc1-dependent manner. 5) MCP-1-induced HASMC growth and migration require NFATc1-dependent cyclin D1 expression and CDK4/6 activities. 6) MCP-1 induced a sustained activation of PKN1, and this effect is mediated by NFATc1-cyclin D1-CDK6 activity. 8) PKN1 activation is needed for both MCP-1-induced HASMC growth and migration. 9) NFAT-mediated PKN1 activation is also required for BI-induced SMC migration, proliferation, and neointima formation. Previously, we have reported that PDGF-BB and thrombin, the receptor tyrosine kinase, and G protein-coupled receptor agonists, respectively, activate NFATc1 in exerting their effects on VSMC growth and migration (20, 21). In elucidating the mechanisms by which NFATc1 mediates VSMC growth and migration, we found that it enhances cyclin D1

expression at transcriptional levels in HASMCs (23). In accordance with these observations, we also demonstrated that NFAT activation is required for injury-induced SMC migration, proliferation, and neointima formation (22–24). Besides these reports, we found that MCP-1 is produced in an endothelium-denuded artery and mediates injury-induced neointima forma-

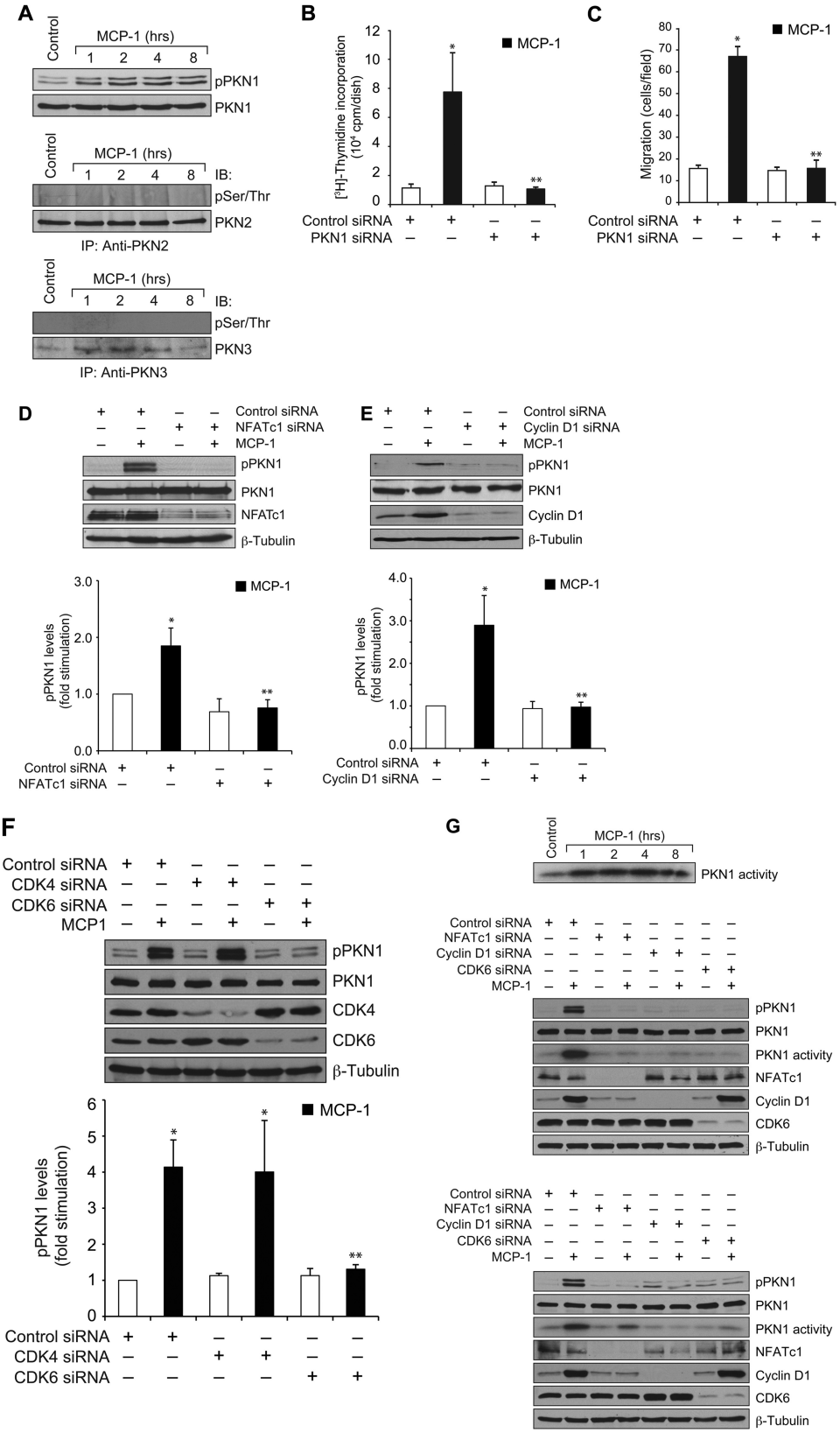

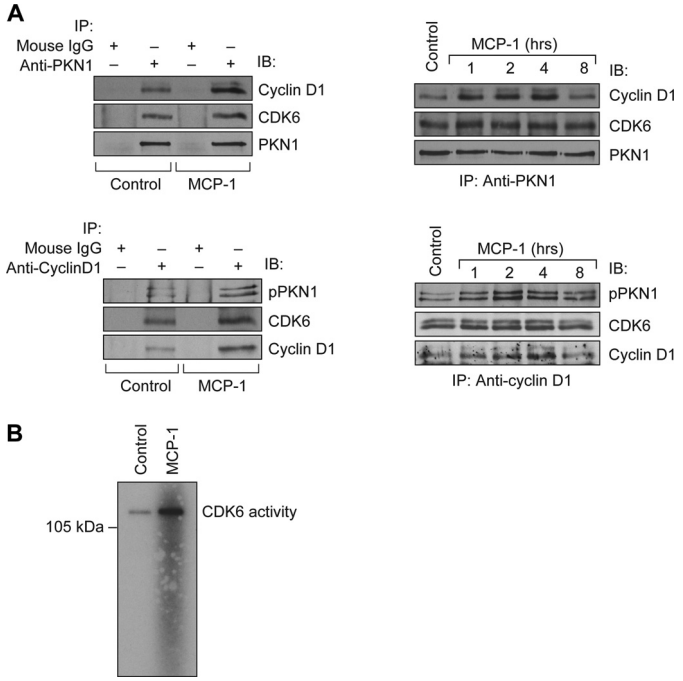

FIGURE 6. **CDK6 phosphorylates PKN1 *in vitro*.** *A,* quiescent HASMCs were treated with and without MCP-1 (50 ng/ml) for the indicated time periods or 8 h, and cell extracts were prepared. An equal amount of protein from control and each treatment was immunoprecipitated (*IP*) with normal IgG, anti-PKN1, or anti-cyclin D1 antibodies, and the immunocomplexes were immunoblotted (*IB*) with anti-cyclin D1, anti-CDK6, anti-pPKN1, and anti-PKN1 antibodies to show their complex formation. *B,* equal amount of protein from control and 8 h of MCP-1-treated HASMCs was immunoprecipitated with anti-CDK6 antibodies, and the immunocomplexes were subjected to immunocomplex kinase assay using recombinant full-length PKN1 and [γ-^{32}P]ATP as substrates.

tion (12). To find out whether NFATc1 is a common effector transcriptional factor in mediating vascular wall remodeling in response to various cues, here we first examined the capacity of MCP-1 in the induction of HASMC growth and migration. MCP-1 induced both HASMC growth and migration. Next, we tested the effect of MCP-1 on NFATc1 activation. MCP-1 not only activated NFATc1 in HASMCs but its stimulation is required for the growth and migration of these cells in response to this chemokine. Another noteworthy observation is that like PDGF-BB, MCP-1 also induced cyclin D1 expression in an NFATc1-dependent manner, and the induction of cyclin D1 expression resulted in increased CDK4 and CDK6 activities. It was observed that both MCP-1-induced HASMC growth and migration exhibited a requirement for cyclin D1 expression and CDK4/6 activities. An established role of cyclin D1-CDK4/6 is their involvement in G_1-S phase transition of a cell in response to a mitogen (39–41). However, in this study, we present evidence that cyclin D1 in concert with both CDK4 and CDK6 activities plays a role in MCP-1-induced HASMC growth as well as migration. Although pRb phosphorylation is the major mechanism of the cyclin D1-CDK4/6 role in cell cycle progression, the intricacies by which these cell cycle-dependent kinases modulate cell migration are less explored. In this aspect, it was reported that cyclin D1/CDK4 by binding to p27Kip1 sequesters it away from the nucleus and promotes cell migration (42, 43). Additional studies have shown that cyclin D1-CDK4 via modulating the phosphorylation of filamin, an actin-binding protein, mediates cell migration (44). Thus, these studies point out that in addition to their conventional substrate, pRb, cyclin D1-CDK4–6 may phosphorylate many other molecules, including cytoskeleton organization proteins, and govern both cell proliferation and migration.

PKN1 is an effector molecule of RhoA/Rac1 and mediates cell migration by phosphorylating cytoskeleton organization proteins (45–47). Besides its role in the regulation of cell migration, two elegant studies in recent years have reported that PKN1 plays a major role in phosphorylation-dependent demethylation of histone H3 and its involvement in chromatin remodeling and gene regulation downstream to androgen receptor activation (48, 49). In exploring the mechanisms by which NFATc1 mediates both VSMC proliferation and migration, we reported that it modulates cyclin D1 expression at a transcriptional level and this in turn results in increased CDK4 activity (23). Toward elucidation of more downstream mechanisms, in this study, as depicted in Fig. 10, we discovered that NFATc1 via enhancing the expression of cyclin D1 and thereby modulating CDK6 activity mediates PKN1 phosphorylation/activation in a sustained manner in response to MCP-1. Because activation of PKN1 appears to be distal to NFATc1-cyclin D1-CDK6, it is more likely that PKN1 is involved in gene regulation downstream to NFATc1 mediating both cell proliferation and migration. One potential mechanism by which PKN1 may be involved in NFATc1-cyclin D1-CDK6-mediated gene regulation could be via phosphorylation-dependent modifications of histones and their involvement in chromatin remodeling. This view also points out an additional role for

FIGURE 5. **MCP-1-induced proliferation and migration require PKN1 activation.** *A,* quiescent HASMCs were treated with and without MCP-1 (50 ng/ml) for the indicated time periods, and cell extracts were prepared and analyzed by Western blotting for pPKN1 levels using its phospho-specific antibodies or immunoprecipitated (*IP*) with anti-PKN2 or anti-PKN3 antibodies followed by immunoblotting (*IB*) with Ser(P)/Thr(P) antibodies. *B* and *C,* HASMCs that were transfected with control or PKN1 siRNA (100 nM) and quiesced were subjected to MCP-1-induced DNA synthesis (*B*) and migration (*C*). *D–F,* HASMCs were transfected with control, cyclin D1, CDK4, CDK6, or NFATc1 siRNA (100 nM), quiesced, and treated with and without MCP-1 (50 ng/ml) for 8 h, and cell extracts were prepared and analyzed by Western blotting for pPKN1 levels using its specific antibodies. The blots in *A* and *D–F* were sequentially reprobed with anti-PKN1, anti-PKN2, anti-PKN3, anti-cyclin D1, anti-CDK4, or anti-CDK6 antibodies to show normalization, lane loading control, or the effect of a specific siRNA on its target and nontarget gene expression. *G, upper panel,* an equal amount of protein from control and the indicated time periods of MCP-1 (50 ng/ml)-treated quiescent HASMCs were analyzed by immunocomplex kinase assay for PKN1 activity using myelin basic protein (MBP) and [γ-^{32}P]ATP as substrates. *Middle panel,* HASMCs that were transfected with control, NFATc1, cyclin D1, or CDK6 siRNA (100 nM) and quiesced were treated with and without MCP-1 (50 ng/ml) for 8 h, and cell extracts were prepared. Cell extracts containing an equal amount of protein from control and each treatment were analyzed for PKN1 activity as described in the *upper panel*. An equal amount of protein from the same cell extracts was also analyzed by Western blotting for pPKN1, PKN1, NFATc1, cyclin D1, CDK6, and β-tubulin levels using their specific antibodies to show the effect of the indicated siRNA on PKN1 phosphorylation as well as their target and nontarget gene expression or normalization. *Bottom panel,* HASMCs that were transfected with control, NFATc1, cyclin D1, or CDK6 siGENOME siRNA (100 nM) and quiesced were treated with and without MCP-1 (50 ng/ml) for 8 h, and cell extracts were prepared. Cell extracts containing an equal amount of protein from control and each treatment were analyzed by immunocomplex kinase assay for PKN1 activity and by Western blotting for pPKN1, PKN1, NFATc1, cyclin D1, CDK6, and β-tubulin levels as described in the *middle panel*. *, $p < 0.01$ *versus* control siRNA; **, $p < 0.01$ *versus* control siRNA + MCP-1.

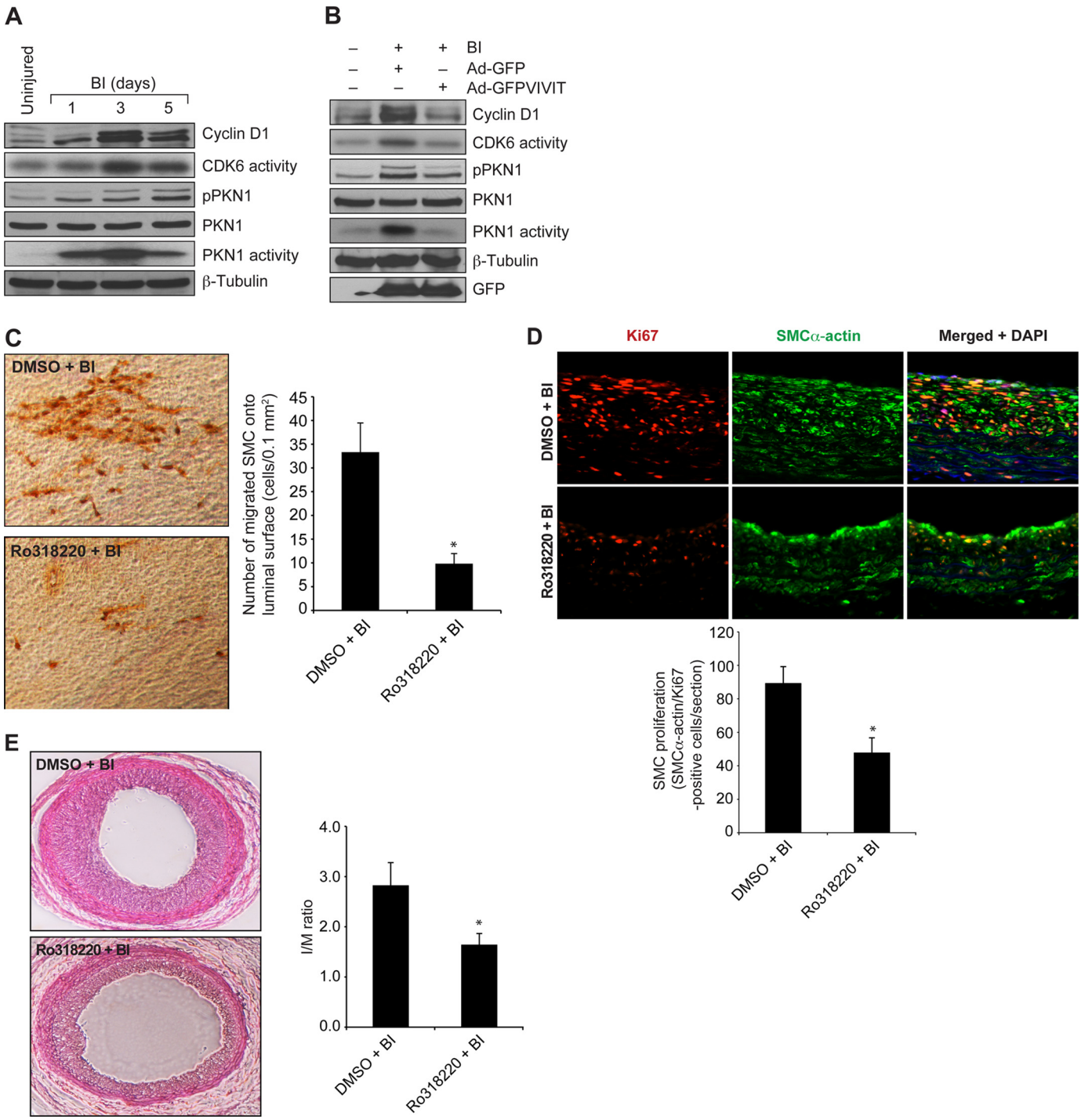

FIGURE 7. **Balloon injury induces PKN1 activation via NFAT-dependent manner and pharmacological inhibition of PKN1 suppresses BI-induced SMC migration, proliferation, and neointima formation.** *A,* common carotid arteries were dissected out after the indicated time periods of BI, and tissue extracts were prepared. The tissue extracts containing an equal amount of protein were analyzed for cyclin D1, pPKN1, PKN1, and β-tubulin levels by Western blotting using their specific antibodies or CDK6 and PKN1 activities by immunocomplex kinase assays. Recombinant retinoblastoma protein was used as a substrate for CDK6 assay, and MBP was used as a substrate for PKN1 assay. *B,* immediately following BI, arteries were transduced with Ad-GFP or Ad-GFPVIVIT at 10^{10} pfu/ml. At 3 days post-BI, arteries were dissected out, and tissue extracts were prepared and analyzed for cyclin D1, pPKN1, PKN1, GFP, and β-tubulin levels by Western blotting or CDK6 and PKN1 activities by immunocomplex kinase assays as described in *A. C,* at 3 days post-BI and administration with vehicle or Ro318220 (10 μM) in 30% pluronic gel, the arteries were isolated, opened longitudinally, and stained with anti-SMCα-actin antibodies. The SMCα-actin-positive cells were counted, and SMC migration was expressed as the number of SMCα-actin-positive cells migrated onto a unit luminal surface area. The *left panel* shows a representative picture of SMC migration onto the luminal surface, and the *bar graph* on the *right* represents the quantitative analysis of SMC migration from six animals. *D,* at 1 week post-BI and exposure to vehicle or Ro318220 (10 μM) in 30% pluronic gel, the arteries were isolated and fixed, and cryosections were made and stained for SMCα-actin and Ki67 using their specific antibodies. The *upper panel* shows the representative pictures of neointimal SMC proliferation, and the *lower bar graph* shows the quantitative analysis of neointimal SMC proliferation from six animals. *E,* at 2 weeks post-BI and exposure to vehicle or Ro318220 (10 μM) in 30% pluronic gel, the arteries were isolated, fixed, cross-sections made, and stained with H&E, and the I/M ratios were calculated. The *left panel* shows the representative pictures of balloon-injured common carotid artery cross-sections that were stained with H&E. The *bar graph* in the *right panel* shows the quantitative analysis of the I/M ratios of the injured common carotid arteries of six animals. *, $p < 0.05$ *versus* DMSO + BI.

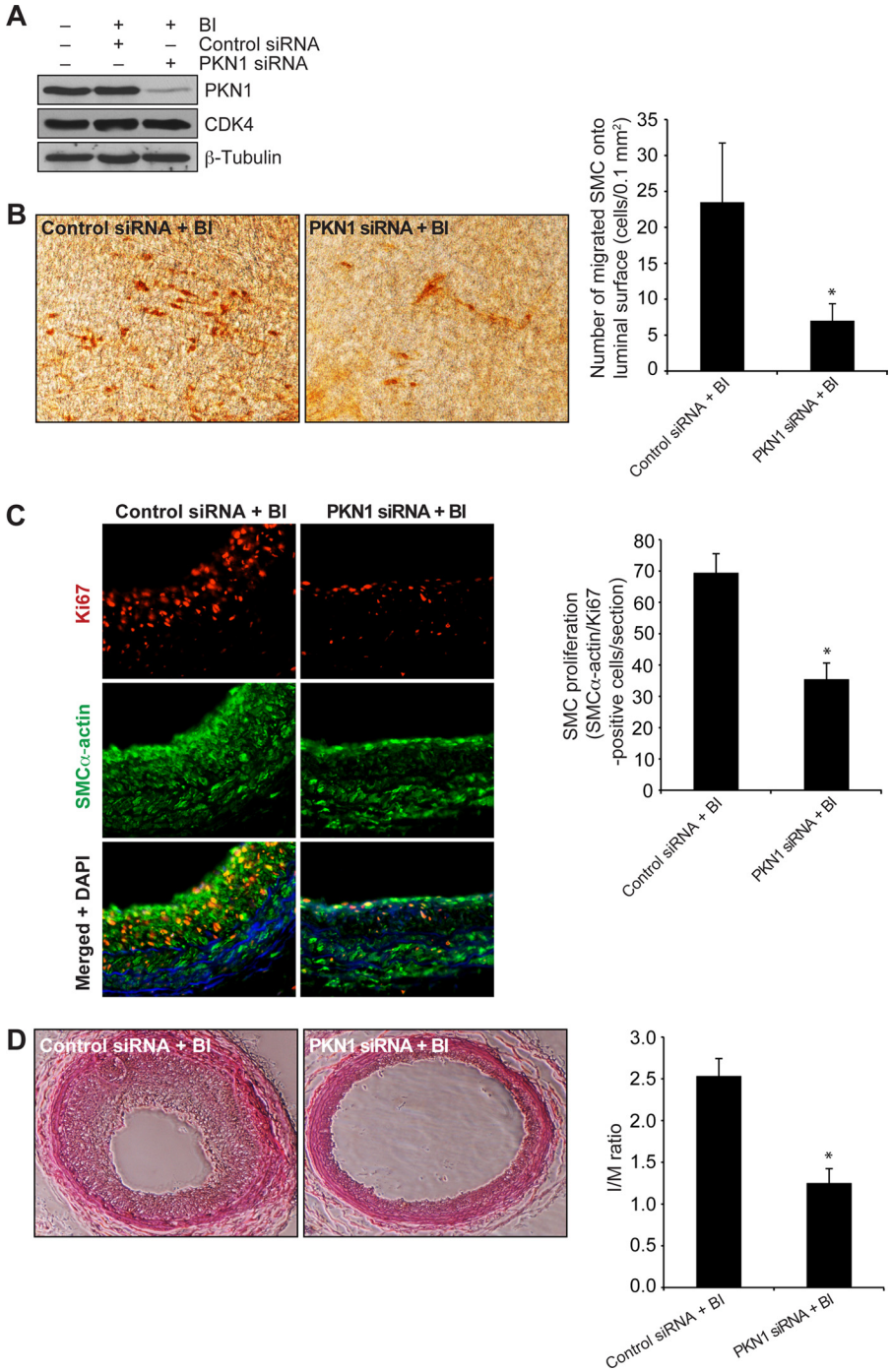

FIGURE 8. **Down-regulation of PKN1 levels inhibits BI-induced SMC migration, proliferation, and neointima formation.** *A,* at 3 days post-BI and administration with 10 μg of control or PKN1 siRNA, injured and uninjured common carotid arteries were isolated, and tissue extracts were prepared and analyzed by Western blotting for PKN1 levels to show its depletion by its siRNA. The blot was reprobed with anti-CDK4 and anti-β-tubulin antibodies for normalization. *B,* all the conditions were the same as in *A* except that injured common carotid arteries were opened longitudinally and stained with anti-SMCα-actin antibodies. SMC migration was expressed as the number of SMCα-actin-positive cells migrated onto a unit luminal surface area. The *left panel* shows a representative picture of SMC migration onto the luminal surface, and the *bar graph* on the *right* represents the quantitative analysis of SMC migration from six animals. *C,* at 1 week post-BI and administration with 10 μg of control or PKN1 siRNA, injured common carotid arteries were isolated and fixed, and cryosections were made and stained for SMCα-actin and Ki67 using their specific antibodies. The *left panel* shows the representative pictures of neointimal SMC proliferation, and the *bar graph* on the *right* shows the quantitative analysis of the neointimal SMC proliferation from six animals. *D,* at 2 weeks post-BI and administration with 10 μg of control or PKN1 siRNA, injured common carotid arteries were isolated and fixed, and cross-sections were made, stained with H&E, and the I/M ratios were calculated. The *left panel* shows the representative pictures of balloon-injured common carotid artery cross-sections that were stained with H&E. The *bar graph* on the *right* shows the quantitative analysis of the I/M ratios of the injured common carotid arteries from six animals. *, $p < 0.05$ *versus* control siRNA + BI.

NFATc1 in chromatin remodeling. Previously, some studies have reported that NFATs are involved in mediating angiogenesis (50, 51). However, the exact mechanisms by which NFATs are involved in angiogenesis are not clear. Based on the present findings, it may be speculated that NFATs, particularly NFATc1, via targeting cyclin D1-CDK4/6 activities and thereby

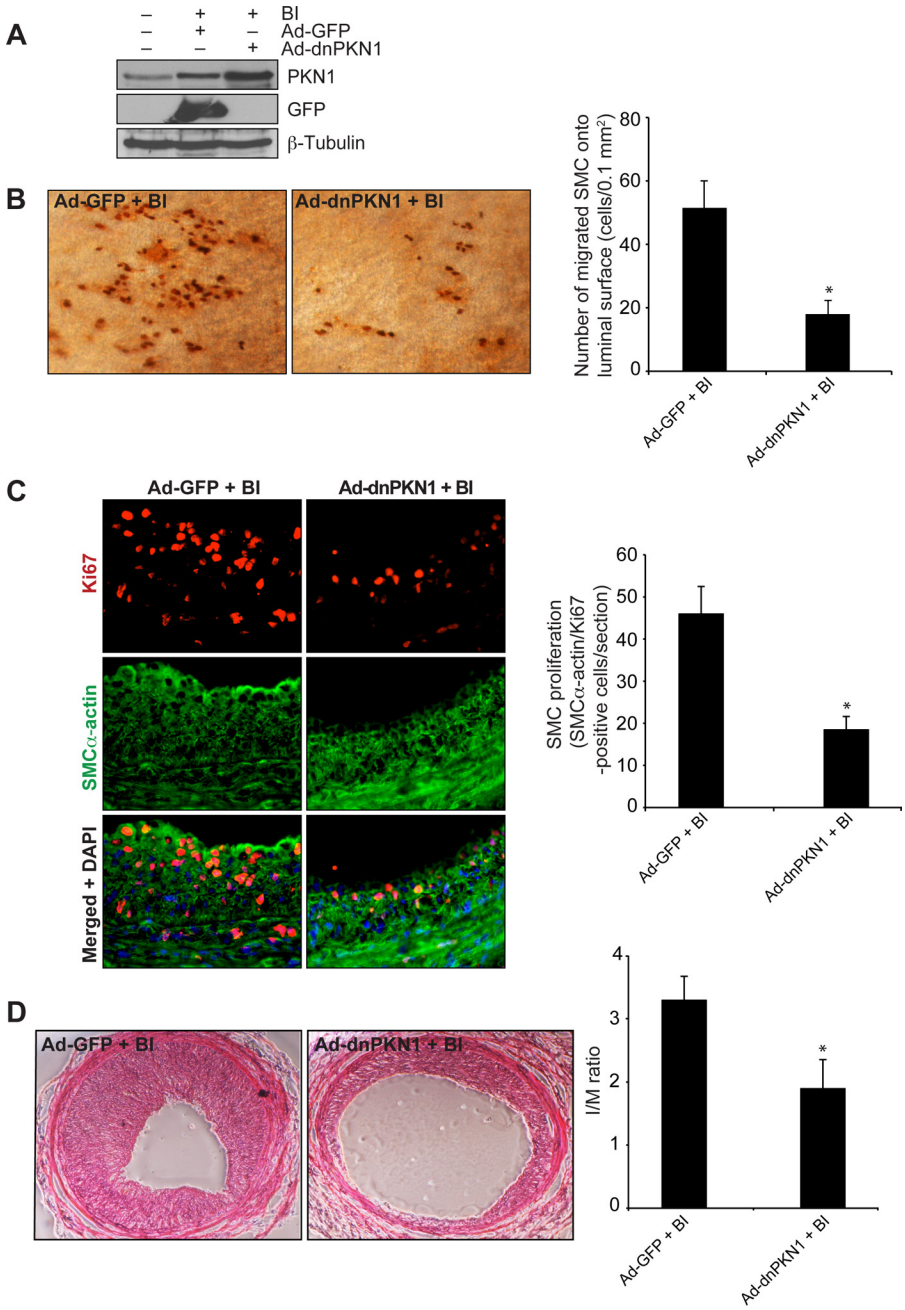

FIGURE 9. **Blockade of PKN1 activation inhibits BI-induced SMC migration, proliferation, and neointima formation.** *A,* at 3 days post-BI and transduction with Ad-GFP or Ad-dnPKN1 (10^9 pfu), injured and uninjured common carotid arteries were isolated and tissue extracts were prepared and analyzed by Western blotting for the overexpression of dnPKN1 or GFP, and one of these blots was reprobed for β-tubulin levels for normalization. *B,* all the conditions were the same as in *A* except that the injured arteries were opened longitudinally and stained with anti-SMCα-actin antibodies. SMC migration was expressed as the number of SMCα-actin-positive cells migrated onto a unit luminal surface area. The *left panel* shows a representative picture of SMC migration onto the luminal surface, and the *bar graph* on the *right* represents the quantitative analysis of SMC migration from six animals. *C,* at 1 week post-BI and transduction with Ad-GFP or Ad-dnPKN1 (10^9 pfu), injured common carotid arteries were isolated and fixed, and cryosections were made and stained for SMCα-actin and Ki67 using their specific antibodies. The *left panel* shows the representative pictures of neointimal SMC proliferation, and the *bar graph* on the *right* shows the quantitative analysis of the neointimal SMC proliferation from six animals. *D,* at 2 weeks post-BI and transduction with Ad-GFP or Ad-dnPKN1 (10^9 pfu), injured common carotid arteries were isolated and fixed, and cross-sections were made, stained with H&E, and the I/M ratios calculated. The *left panel* shows the representative pictures of balloon-injured common carotid artery cross-sections that were stained with H&E. The *bar graph* on the *right* shows the quantitative analysis of the I/M ratios of the injured common carotid arteries from six animals. *, $p < 0.05$ *versus* Ad-GFP + BI.

PKN1 phosphorylation/activation may be involved in the regulation of endothelial cell proliferation and migration, the two important events that are essential for angiogenesis.

The findings that BI induces cyclin D1 expression, CDK6 activity, and PKN1 phosphorylation/activation in an NFAT-dependent manner affirms that a signaling cascade that gets activated in response to a potent chemotactic protein, MCP-1, in HASMCs *in vitro* also occurs in intact artery in response to injury. Previously, we have reported that NFATs mediate BI-induced vascular wall remodeling. In addition, we showed that NFATs target cyclin D1 and thereby CDK4 activity in mediating BI-induced SMC migration and proliferation. In this study,

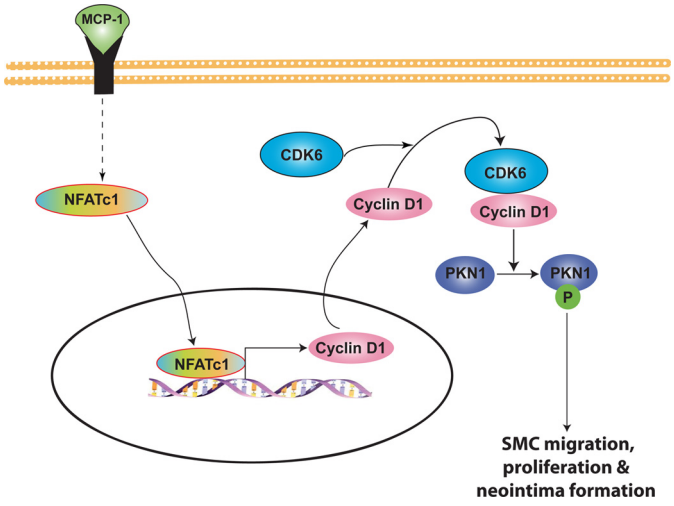

FIGURE 10. **Schematic diagram showing the potential mechanisms of PKN1 activation by MCP-1.**

we identify PKN1 as a new target molecule of NFAT-cyclin D1/CDK6 axis in mediating BI-induced SMC migration and proliferation, leading to enhanced neointima formation. Based on these observations, PKN1 could be a novel target for the drug development for cardiovascular diseases such as restenosis.

REFERENCES

1. Schwartz, S. M., deBlois, D., and O'Brien, E. R. (1995) The intima. Soil for atherosclerosis and restenosis. *Circ. Res.* **77,** 445–465
2. Berk, B. C. (2001) Vascular smooth muscle growth. Autocrine growth mechanisms. *Physiol. Rev.* **81,** 999–1030
3. Kumar, A. H., Metharom, P., Schmeckpeper, J., Weiss, S., Martin, K., and Caplice, N. M. (2010) Bone marrow-derived CX3CR1 progenitors contribute to neointimal smooth muscle cells via fractalkine CX3CR1 interaction. *FASEB J.* **24,** 81–92
4. Furukawa, Y., Matsumori, A., Ohashi, N., Shioi, T., Ono, K., Harada, A., Matsushima, K., and Sasayama, S. (1999) Anti-monocyte chemoattractant protein-1/monocyte chemotactic and activating factor antibody inhibits neointimal hyperplasia in injured rat carotid arteries. *Circ. Res.* **84,** 306–314
5. Carr, M. W., Roth, S. J., Luther, E., Rose, S. S., and Springer, T. A. (1994) Monocyte chemoattractant protein 1 acts as a T-lymphocyte chemoattractant. *Proc. Natl. Acad. Sci. U.S.A.* **91,** 3652–3656
6. Xu, L. L., Warren, M. K., Rose, W. L., Gong, W., and Wang, J. M. (1996) Human recombinant monocyte chemotactic protein and other C-C chemokines bind and induce directional migration of dendritic cells *in vitro*. *J. Leukocyte Biol.* **60,** 365–371
7. Ikeda, U., Okada, K., Ishikawa, S., Saito, T., Kasahara, T., and Shimada, K. (1995) Monocyte chemoattractant protein 1 inhibits growth of rat vascular smooth muscle cells. *Am. J. Physiol.* **268,** H1021–H1026
8. Tieu, B. C., Lee, C., Sun, H., Lejeune, W., Recinos, A., 3rd, Ju, X., Spratt, H., Guo, D. C., Milewicz, D., Tilton, R. G., and Brasier, A. R. (2009) An adventitial IL-6/MCP1 amplification loop accelerates macrophage-mediated vascular inflammation leading to aortic dissection in mice. *J. Clin. Invest.* **119,** 3637–3651
9. Zhang, F., Tsai, S., Kato, K., Yamanouchi, D., Wang, C., Rafii, S., Liu, B., and Kent, K. C. (2009) Transforming growth factor-β promotes recruitment of bone marrow cells and bone marrow-derived mesenchymal stem cells through stimulation of MCP-1 production in vascular smooth muscle cells. *J. Biol. Chem.* **284,** 17564–17574
10. Spinetti, G., Wang, M., Monticone, R., Zhang, J., Zhao, D., and Lakatta, E. G. (2004) Rat aortic MCP-1 and its receptor CCR2 increase with age and alter vascular smooth muscle cell function. *Arterioscler. Thromb. Vasc. Biol.* **24,** 1397–1402
11. Singh, N. K., Wang, D., Kundumani-Sridharan, V., Van Quyen, D., Niu, J., and Rao, G. N. (2011) 15-Lipoxygenase-1-enhanced Src-Janus kinase 2-signal transducer and activator of transcription 3 stimulation and monocyte chemoattractant protein-1 expression require redox-sensitive activation of epidermal growth factor receptor in vascular wall remodeling. *J. Biol. Chem.* **286,** 22478–22488
12. Potula, H. S., Wang, D., Quyen, D. V., Singh, N. K., Kundumani-Sridharan, V., Karpurapu, M., Park, E. A., Glasgow, W. C., and Rao, G. N. (2009) Src-dependent STAT-3-mediated expression of monocyte chemoattractant protein-1 is required for 15(*S*)-hydroxyeicosatetraenoic acid-induced vascular smooth muscle cell migration. *J. Biol. Chem.* **284,** 31142–31155
13. Hogan, P. G., Chen, L., Nardone, J., and Rao, A. (2003) Transcriptional regulation by calcium, calcineurin, and NFAT. *Genes Dev.* **17,** 2205–2232
14. Loh, C., Shaw, K. T., Carew, J., Viola, J. P., Luo, C., Perrino, B. A., and Rao, A. (1996) Calcineurin binds the transcription factor NFAT1 and reversibly regulates its activity. *J. Biol. Chem.* **271,** 10884–10891
15. Chow, W., Hou, G., and Bendeck, M. P. (2008) Glycogen synthase kinase 3β regulation of nuclear factor of activated T-cells isoform c1 in the vascular smooth muscle cell response to injury. *Exp. Cell Res.* **314,** 2919–2929
16. Graef, I. A., Chen, F., Chen, L., Kuo, A., and Crabtree, G. R. (2001) Signals transduced by Ca^{2+}/calcineurin and NFATc3/c4 pattern the developing vasculature. *Cell* **105,** 863–875
17. Horsley, V., Friday, B. B., Matteson, S., Kegley, K. M., Gephart, J., and Pavlath, G. K. (2001) Regulation of the growth of multinucleated muscle cells by an NFATC2-dependent pathway. *J. Cell Biol.* **153,** 329–338
18. Molkentin, J. D., Lu, J. R., Antos, C. L., Markham, B., Richardson, J., Robbins, J., Grant, S. R., and Olson, E. N. (1998) A calcineurin-dependent transcriptional pathway for cardiac hypertrophy. *Cell* **93,** 215–228
19. Ranger, A. M., Grusby, M. J., Hodge, M. R., Gravallese, E. M., de la Brousse, F. C., Hoey, T., Mickanin, C., Baldwin, H. S., and Glimcher, L. H. (1998) The transcription factor NF-ATc is essential for cardiac valve formation. *Nature* **392,** 186–190
20. Liu, Z., Dronadula, N., and Rao, G. N. (2004) A novel role for nuclear factor of activated T cells in receptor tyrosine kinase and G protein-coupled receptor agonist-induced vascular smooth muscle cell motility. *J. Biol. Chem.* **279,** 41218–41226
21. Yellaturu, C. R., Ghosh, S. K., Rao, R. K., Jennings, L. K., Hassid, A., and Rao, G. N. (2002) A potential role for nuclear factor of activated T-cells in receptor tyrosine kinase and G-protein-coupled receptor agonist-induced cell proliferation. *Biochem. J.* **368,** 183–190
22. Liu, Z., Zhang, C., Dronadula, N., Li, Q., and Rao, G. N. (2005) Blockade of nuclear factor of activated T cell activation signaling suppresses balloon injury-induced neointima formation in a rat carotid artery model. *J. Biol. Chem.* **280,** 14700–14708
23. Karpurapu, M., Wang, D., Van Quyen, D., Kim, T. K., Kundumani-Sridharan, V., Pulusani, S., and Rao, G. N. (2010) Cyclin D1 is a *bona fide* target gene of NFATc1 and is sufficient in the mediation of injury-induced vascular wall remodeling. *J. Biol. Chem.* **285,** 3510–3523
24. Karpurapu, M., Wang, D., Singh, N. K., Li, Q., and Rao, G. N. (2008) NFATc1 targets cyclin A in the regulation of vascular smooth muscle cell multiplication during restenosis. *J. Biol. Chem.* **283,** 26577–26590
25. Gotoh, Y., Oishi, K., Shibata, H., Yamagiwa, A., Isagawa, T., Nishimura, T., Goyama, E., Takahashi, M., Mukai, H., and Ono, Y. (2004) Protein kinase PKN1 associates with TRAF2 and is involved in TRAF2-NF-κB signaling pathway. *Biochem. Biophys. Res. Commun.* **314,** 688–694
26. Kundumani-Sridharan, V., Wang, D., Karpurapu, M., Liu, Z., Zhang, C., Dronadula, N., and Rao, G. N. (2007) Suppression of activation of signal transducer and activator of transcription-5B signaling in the vessel wall reduces balloon injury-induced neointima formation. *Am. J. Pathol.* **171,** 1381–1394
27. Isagawa, T., Takahashi, M., Kato, T., Jr., Mukai, H., and Ono, Y. (2005) Involvement of protein kinase PKN1 in G_2/M delay caused by arsenite. *Mol. Carcinog.* **43,** 1–12
28. Rao, G. N., Katki, K. A., Madamanchi, N. R., Wu, Y., and Birrer, M. J. (1999) JunB forms the majority of the AP-1 complex and is a target for redox regulation by receptor tyrosine kinase and G protein-coupled receptor agonists in smooth muscle cells. *J. Biol. Chem.* **274,** 6003–6010
29. Dronadula, N., Rizvi, F., Blaskova, E., Li, Q., and Rao, G. N. (2006) Involve-

ment of cAMP-response element-binding protein-1 in arachidonic acid-induced vascular smooth muscle cell motility. *J. Lipid Res.* **47,** 767–777
30. Wang, D., Liu, Z., Li, Q., Karpurapu, M., Kundumani-Sridharan, V., Cao, H., Dronadula, N., Rizvi, F., Bajpai, A. K., Zhang, C., Müller-Newen, G., Harris, K. W., and Rao, G. N. (2007) An essential role for gp130 in neointima formation following arterial injury. *Circ. Res.* **100,** 807–816
31. Subramanian, P., Karshovska, E., Reinhard, P., Megens, R. T., Zhou, Z., Akhtar, S., Schumann, U., Li, X., van Zandvoort, M., Ludin, C., Weber, C., and Schober, A. (2010) Lysophosphatidic acid receptors LPA1 and LPA3 promote CXCL12-mediated smooth muscle progenitor cell recruitment in neointima formation. *Circ. Res.* **107,** 96–105
32. Bendeck, M. P., Zempo, N., Clowes, A. W., Galardy, R. E., and Reidy, M. A. (1994) Smooth muscle cell migration and matrix metalloproteinase expression after arterial injury in the rat. *Circ. Res.* **75,** 539–545
33. Aramburu, J., Yaffe, M. B., López-Rodríguez, C., Cantley, L. C., Hogan, P. G., and Rao, A. (1999) Affinity-driven peptide selection of an NFAT inhibitor more selective than cyclosporin A. *Science* **285,** 2129–2133
34. Heasman, S. J., and Ridley, A. J. (2008) Mammalian Rho GTPases. New insights into their functions from *in vivo* studies. *Nat. Rev. Mol. Cell Biol.* **9,** 690–701
35. Bokoch, G. M. (2005) Regulation of innate immunity by Rho GTPases. *Trends Cell Biol.* **15,** 163–171
36. Gampel, A., Parker, P. J., and Mellor, H. (1999) Regulation of epidermal growth factor receptor traffic by the small GTPase RhoB. *Curr. Biol.* **9,** 955–958
37. Mukai, H. (2003) The structure and function of PKN, a protein kinase having a catalytic domain homologous to that of PKC. *J. Biochem.* **133,** 17–27
38. Standaert, M., Bandyopadhyay, G., Galloway, L., Ono, Y., Mukai, H., and Farese, R. (1998) Comparative effects of GTPγS and insulin on the activation of Rho, phosphatidylinositol 3-kinase, and protein kinase N in rat adipocytes. Relationship to glucose transport. *J. Biol. Chem.* **273,** 7470–7477
39. Sherr, C. J., and Roberts, J. M. (2004) Living with or without cyclins and cyclin-dependent kinases. *Genes Dev.* **18,** 2699–2711
40. Weinberg, R. A. (1995) The retinoblastoma protein and cell cycle control. *Cell* **81,** 323–330
41. Baldin, V., Lukas, J., Marcote, M. J., Pagano, M., and Draetta, G. (1993) Cyclin D1 is a nuclear protein required for cell cycle progression in G_1. *Genes Dev.* **7,** 812–821
42. Larrea, M. D., Hong, F., Wander, S. A., da Silva, T. G., Helfman, D., Lannigan, D., Smith, J. A., and Slingerland, J. M. (2009) RSK1 drives p27Kip1 phosphorylation at T198 to promote RhoA inhibition and increase cell motility. *Proc. Natl. Acad. Sci. U.S.A.* **106,** 9268–9273
43. Li, Z., Jiao, X., Wang, C., Ju, X., Lu, Y., Yuan, L., Lisanti, M. P., Katiyar, S., and Pestell, R. G. (2006) Cyclin D1 induction of cellular migration requires p27(KIP1). *Cancer Res.* **66,** 9986–9994
44. Zhong, Z., Yeow, W. S., Zou, C., Wassell, R., Wang, C., Pestell, R. G., Quong, J. N., and Quong, A. A. (2010) Cyclin D1/cyclin-dependent kinase 4 interacts with filamin A and affects the migration and invasion potential of breast cancer cells. *Cancer Res.* **70,** 2105–2114
45. Turner, E. C., Kavanagh, D. J., Mulvaney, E. P., McLean, C., Wikström, K., Reid, H. M., and Kinsella, B. T. (2011) Identification of an interaction between the TPα and TPβ isoforms of the human thromboxane A_2 receptor with protein kinase C-related kinase (PRK) 1. Implications for prostate cancer. *J. Biol. Chem.* **286,** 15440–15457
46. Owen, D., Lowe, P. N., Nietlispach, D., Brosnan, C. E., Chirgadze, D. Y., Parker, P. J., Blundell, T. L., and Mott, H. R. (2003) Molecular dissection of the interaction between the small G proteins Rac1 and RhoA and protein kinase C-related kinase 1 (PRK1). *J. Biol. Chem.* **278,** 50578–50587
47. Flynn, P., Mellor, H., Casamassima, A., and Parker, P. J. (2000) Rho GTPase control of protein kinase C-related protein kinase activation by 3-phosphoinositide-dependent protein kinase. *J. Biol. Chem.* **275,** 11064–11070
48. Metzger, E., Imhof, A., Patel, D., Kahl, P., Hoffmeyer, K., Friedrichs, N., Müller, J. M., Greschik, H., Kirfel, J., Ji, S., Kunowska, N., Beisenherz-Huss, C., Günther, T., Buettner, R., and Schüle, R. (2010) Phosphorylation of histone H3T6 by PKCβ(I) controls demethylation at histone H3K4. *Nature* **464,** 792–796
49. Metzger, E., Yin, N., Wissmann, M., Kunowska, N., Fischer, K., Friedrichs, N., Patnaik, D., Higgins, J. M., Potier, N., Scheidtmann, K. H., Buettner, R., and Schüle, R. (2008) Phosphorylation of histone H3 at threonine 11 establishes a novel chromatin mark for transcriptional regulation. *Nat. Cell Biol.* **10,** 53–60
50. Urso, K., Alfranca, A., Martínez-Martínez, S., Escolano, A., Ortega, I., Rodríguez, A., and Redondo, J. M. (2011) NFATc3 regulates the transcription of genes involved in T-cell activation and angiogenesis. *Blood* **118,** 795–803
51. Mancini, M., and Toker, A. (2009) NFAT proteins. Emerging roles in cancer progression. *Nat. Rev. Cancer* **9,** 810–820